ARTICLE

OBC
www.rsc.org/obc

NMR studies of interactions between periplasmic chaperones from uropathogenic *E. coli* and pilicides that interfere with chaperone function and pilus assembly

Mattias Hedenström,[a] Hans Emtenäs,[b] Nils Pemberton,[a] Veronica Åberg,[a] Scott J. Hultgren,[c] Jerome S. Pinkner,[c] Viola Tegman,[d] Fredrik Almqvist,[a] Ingmar Sethson[a] and Jan Kihlberg*[a,b]

[a] *Organic Chemistry, Department of Chemistry, Umeå University, SE-901 87, Umeå, Sweden. E-mail: jan.kihlberg@chem.umu.se*

[b] *AstraZeneca R & D, SE-431 83, Mölndal, Sweden*

[c] *Department of Molecular Microbiology, Washington University School of Medicine, 660 South Euclid Avenue, St. Louis, MO 63110, USA*

[d] *Biochemistry, Department of Chemistry, Umeå University, SE-901 87, Umeå, Sweden*

Received 23rd August 2005, Accepted 5th October 2005
First published as an Advance Article on the web 31st October 2005

Adherence of uropathogenic *Escherichia coli* to host tissue is mediated by pili, which are hair-like protein structures extending from the outer cell membrane of the bacterium. The chaperones FimC and PapD are key components in pilus assembly since they catalyse folding of subunits that are incorporated in type 1 and P pili, respectively, and also transport the subunits across the periplasmic space. Recently, compounds that inhibit pilus biogenesis and interfere with chaperone–subunit interactions have been discovered and termed pilicides. In this paper NMR spectroscopy was used to study the interaction of different pilicides with PapD and FimC in order to gain structural knowledge that would explain the effect that some pilicides have on pilus assembly. First relaxation-edited NMR experiments revealed that the pilicides bound to the PapD chaperone with mM affinity. Then the pilicide–chaperone interaction surface was investigated through chemical shift mapping using ^{15}N-labelled FimC. Principal component analysis performed on the chemical shift perturbation data revealed the presence of three binding sites on the surface of FimC, which interacted with three different classes of pilicides. Analysis of structure–activity relationships suggested that pilicides reduce pilus assembly in *E. coli* either by binding in the cleft of the chaperone, or by influencing the orientation of the flexible F1–G1 loop, both of which are part of the surface by which the chaperone forms complexes with pilus subunits. It is suggested that binding to either of these sites interferes with folding of the pilus subunits, which occurs during formation of the chaperone–subunit complexes. In addition, pilicides that influence the F1–G1 loop also appear to reduce pilus formation by their ability to dissociate chaperone–subunit complexes.

Introduction

Pili are rod-like, oligomeric extracellular protein fibres formed by a wide range of pathogenic bacteria.[1] Their function is to allow bacteria to adhere to the epithelial surface of the host in order to facilitate invasion and colonization of the underlying tissue. Uropathogenic *Escherichia coli* forms two kinds of pili, type 1 pili and P pili, that are involved in development of different forms of urinary tract infections (UTIs). For type 1 pili the rod consists of repeating FimA subunits ending with a short fibrillum having the adhesin FimH[2] at the tip. FimH binds to mannose oligosaccharides present on the epithelial cells in the bladder;[3] a binding that is critical for development of UTI in the bladder (cystitis). P pili are constructed in a similar fashion with a rod consisting of repeating PapA subunits and a tip fibrillum containing the adhesin PapG as well as three other pilus-proteins.[4] This adhesin binds to the Galα(1–4)Gal disaccharide found in glycolipids in the upper urinary tract,[5–7] thereby allowing the infection to ascend into the kidneys (pyelonephritis).

Pilus biogenesis proceeds *via* the chaperone–usher pathway,[8] in which the periplasmic chaperones FimC and PapD play a crucial role in formation of type 1 and P pili, respectively. The two chaperones have almost identical secondary and tertiary structures and each consists of two domains with an immunoglobulin (Ig)-like fold.[9,10] The domains are oriented so that a cleft is formed between them, giving the chaperones an overall boomerang-like shape. The close structural relationship between FimC and PapD is reflected by the fact that they may be interchanged, *i.e.* PapD can substitute for FimC in building up type 1 pili.[11] The subunits that make up pili in uropathogenic *E. coli* also have an Ig-like fold but lack one β-strand, thereby exposing a hydrophobic groove, which renders them unstable in their monomeric form. The PapD and FimC chaperones mediate folding[12,13] of the pilus subunits after translocation across the inner cell membrane and then stabilize their structures by forming a complex in the periplasm through a mechanism called donor-strand complementation.[14,15] In the complex, the G1 β-strand of the chaperone complements the missing β-strand in the subunit in a parallel fashion. In addition, a salt-bridge is formed between the C-terminus of the subunit and two conserved residues, Arg8 and Lys112, located in the cleft between the two domains of the chaperone. These key interactions are formed in the same manner in the chaperone–subunit complexes of both type 1[14] and P pili.[15] After formation, the chaperone–subunit complex is transported through the periplasm to an usher in the outer cell membrane of the bacterium, where the pilus is formed through a mechanism called donor-strand exchange.[16] The details of this mechanism are not fully understood but the end result is formation of subunit–subunit interactions through displacement of the chaperone G1 β-strand from the subunit groove by the N-terminal part of the subunit in the next chaperone–subunit complex to approach the usher. As a consequence the chaperone is not incorporated in the pilus.

Inhibition of complex formation between periplasmic chaperones and pilus subunits is an attractive target for new antibacterial drugs. This would interfere with pilus biogenesis and thereby prevent the bacteria from adhering to host tissue without killing

DOI:10.1039/b511857c

them. Based on the structural knowledge of the chaperone–subunit interactions, *vide supra*, a number of different small organic molecules, so called pilicides, have been designed and synthesized.[17–20] The pilicides were designed to bind in the cleft formed by the two domains of FimC and PapD by mimicking the C-terminal part of the subunits,[18,21] thus blocking the chaperone from binding to the pilus subunits in the periplasm. Surface plasmon resonance studies have shown that the pilicides bind specifically to the FimC and PapD chaperones.[18,19] As was expected in view of the close structural similarity between these two chaperones, the pilicides did not discriminate between PapD and FimC. Some of the more potent pilicides were also found to disrupt chaperone–subunit complexes.[18] Moreover, the most potent ones prevented pilus assembly in uropathogenic *E. coli*, as revealed by hemagglutination studies. In the present study we have investigated the structural details of chaperone–pilicide interactions by using nuclear magnetic resonance spectroscopy. Our aims were to estimate the affinity of chaperone–pilicide complexes, to locate the binding site(s) of pilicides on chaperones and to gain knowledge about the mechanism by which pilicides inhibit pilus assembly in *E. coli*.

Results and discussion

Selection of pilicides

A number of pilicides have been designed and synthesized[17–23] based on the crystal structure of the C-terminal peptide from the pilus adhesin PapG in the complex with the PapD chaperone.[24] The collection of pilicides selected for the present study consisted of three different classes; disubstituted pyridones **1–4** and **8**, aminomethylated pyridones **5–7**, and tyrosine derivatives **9** and **10** (Fig. 1). They have all been shown to bind to the FimC and PapD chaperones using surface plasmon resonance,[18,19] except for **8** which was included as a negative control in the chemical shift mapping study discussed below. In addition, computer based modelling suggested that they would bind in the cleft formed by the two domains of the chaperones.[18] Peptide **11**, which is the C-terminal 7-mer from the PapG subunit is known to bind to both chaperones[18] and was included as a positive control in the chemical shift mapping study.

Relaxation-edited NMR experiments and affinity estimation

In order to verify that the pilicides have an affinity for the periplasmic chaperones, relaxation-edited one dimensional ^{1}H NMR experiments[25] were performed with pilicides **1–7** and **9**. PapD, which can readily be produced in larger amounts than FimC, was used in this study. A cpmg spin lock ($90_x - [\tau - 180_y - \tau]_n$) with a total length of 200 ms was used to discriminate between free pilicide and pilicide bound to PapD. Thus, a reduction of the signals emanating from the pilicide upon addition of PapD indicated binding to the chaperone. 1-Naphthylacetic acid, which does not bind to PapD, was used as a negative control in these experiments. The relaxation-edited NMR studies confirmed that all of the studied pilicides, *i.e.* **1–7** and **9**, bound to the PapD chaperone to various extents (*cf.* Fig. 2 for an example).

An estimate of the dissociation constants for the complexes between PapD and pilicides **1–3** and **5–7** was obtained by measuring the T_2 relaxation times of the pilicides in the absence and presence of one equivalent of PapD. The pilicides appear to be in the region of fast exchange on the NMR timescale when switching between the free and bound state since chemical shift changes and line broadenings were observed for some proton resonances upon addition of the chaperone. The dissociation constant was found to be in the low millimolar range (1–10 mM) for pilicides **2**, **3**, and **5–7**, with disubstituted pyridone **1** displaying a somewhat higher affinity (K_d 0.4 mM). These values should only be looked upon as estimates since surface plasmon resonance (unpublished results), ^{19}F NMR spectroscopy of

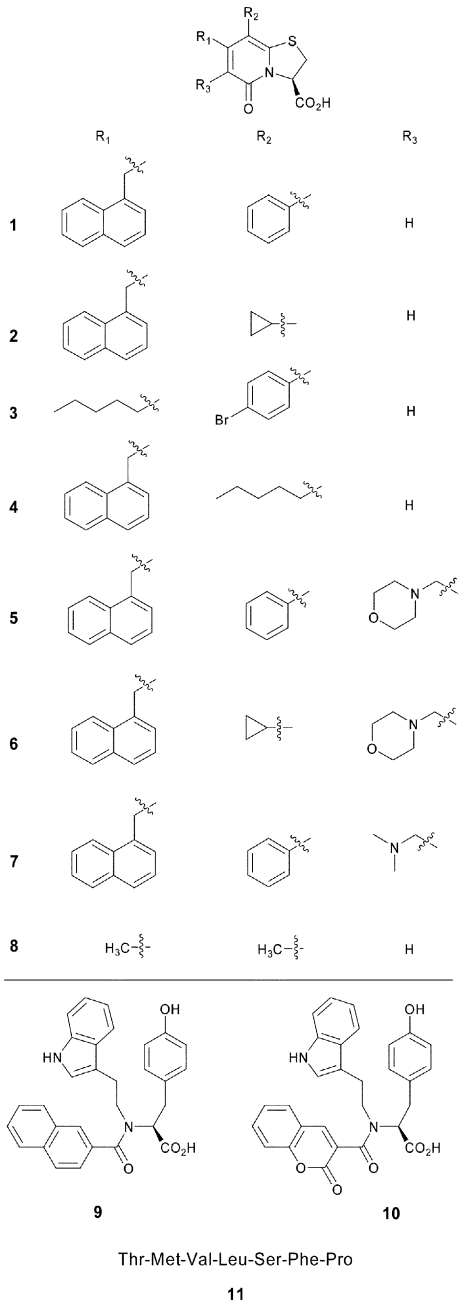

Fig. 1 Ten pilicides selected for NMR studies. Pilicides **1–8** are based on the 2-pyridone scaffold, **9** and **10** are tyrosine derivatives. Peptide **11** is the C-terminal heptamer peptide from the PapG adhesin.

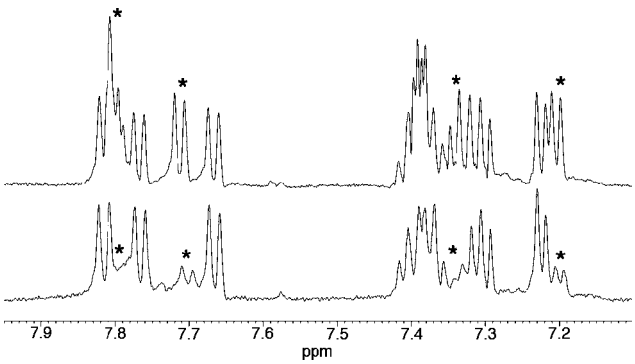

Fig. 2 Relaxation-edited NMR spectra of pilicide **2**. The upper spectrum shows the aromatic region of a 1 : 1 mixture of **2** and 1-naphthylacetic acid. The lower spectrum shows the same region when one equivalent of PapD is present. Peaks marked with an asterisk originate from **2**.

PapD–pilicide complexes[26] as well as the chemical shift mapping data discussed below, suggest the possibility of multiple binding sites for pilicides binding to PapD and FimC.

Chemical shift mapping

Information regarding the location of the pilicide binding site(s) on the surface of the chaperones would be highly valuable in order to obtain a structural understanding of how some pilicides prevent pilus assembly. Such structural information is also essential for the design of subsequent generations of pilicides in efforts to develop improved compounds with potential for use as novel antibacterial agents. Observation of chemical shift perturbations of the backbone amide groups upon complex formation is a strategy that has proved to be valuable for determination of the interaction surface of proteins in complexes with small, drug-like compounds[27] as well as large biomolecules such as RNA[28,29] and other proteins.[30] FimC is the chaperone of choice for such studies since a complete assignment of FimC has been reported.[31] However, two mutations that necessitated a partial reassignment of the backbone were found in the primary structure of FimC, expressed and purified in our laboratory, as compared to the previously assigned structure (Glu18 → Val and Thr174 → Ala). This reassignment was accomplished by a combination of CBCANH[32] and CBCA(CO)NH[33,34] experiments in conjunction with the previously reported FimC assignment. It is important to point out that both of these mutations are positioned well away from the interaction surface between FimC and its subunits, and they should therefore not alter the chaperone's ability to bind pilicides that interfere with pilus assembly.

The C-terminal peptide from a type 1 pilus subunit, such as the adhesin FimH, would serve as a good positive control for chemical shift mapping experiments with ^{15}N-labelled FimC. However, due to the poor solubility of C-terminal peptides from FimH, the C-terminal heptamer peptide from the P pilus adhesin PapG (**11**, Fig. 1) was used instead. Surface plasmon resonance has shown that this peptide binds as well to FimC as the C-terminal heptamer peptide from FimH.[18] The magnitude of the chemical shift changes induced for each backbone amide group of FimC upon addition of one equivalent of **11**, or each of the pilicides, was measured as a weighted average between the shift change in the ^{1}H- and the ^{15}N-dimensions (hereafter referred to as the Δ-values, *cf.* equation in experimental section). The largest effects of peptide binding were found for the backbone amide groups of Arg8 and Lys112 in FimC (Fig. 3). Large portions of the G1 β-strand (residues 101–111), as well as the adjacent F1 β-strand (residues 84–86), also showed major effects, together with some residues in the C-terminal domain close to the interdomain cleft (residues 164, 191–193). These results are in excellent agreement with what would be expected if **11** and FimC formed a complex that had a structure identical to that found in the crystalline FimC–FimH chaperone–pilus adhesin complex,[14] and also in the co-crystal of **11** and PapD.[24]

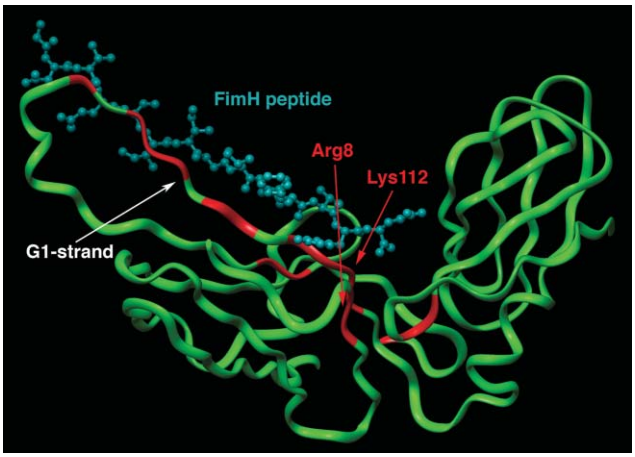

Fig. 3 Part of the crystal structure of the FimC–FimH complex (FimC in green). From the FimH adhesin, only the C-terminal heptamer peptide (blue) is shown. The FimC chaperone is shown in green with residues experiencing a significant shift change ($\Delta > 0.055$) in the presence of the C-terminal heptamer peptide from the PapG adhesin (**11**) marked in red.

The poor solubility of pilicides **1–4** and **8** made it necessary to investigate their binding to FimC in the presence of 5% DMSO. Consequently, the spectra from the samples of these pilicides were compared to a reference spectrum of FimC containing the same amount of DMSO. Judging from the chemical shifts of the backbone amides, this concentration of DMSO has no effect on the structure of the chaperone. Small, relatively hydrophobic compounds such as **1–10** probably interact mainly with the side-chains of FimC. Therefore, it was not unexpected that the chemical shift changes induced by the pilicides were smaller than those induced by the PapG-peptide. The low (mM) affinity estimated for binding of the pilicides to FimC should also contribute to the small shift changes since it results in the fraction of bound pilicide in our experiments being low (0.2–15%). Initially, this raised the question whether the observed shift changes originated from variations in sample preparations, or from other sources beside pilicide–chaperone interactions. However, the fact that no chemical shift changes were observed for the negative control **8**, which binds very weakly to FimC according to surface plasmon resonance, reassured us that the observed chemical shift changes indeed stems from pilicide–chaperone interactions. In addition, pH measurements confirmed that no significant changes in pH (less than 0.02 units) occurred upon addition of pilicide to the FimC samples.

With the exception of the non-binder **8**, the pilicides, as well as peptide **11**, affect a larger portion of the FimC backbone than expected from a single binding site (Fig. 4). There are several plausible explanations for this unexpected result, the most obvious one being that secondary, low affinity binding sites are present on the surface of FimC. This has been indicated previously for some of the pilicides by surface plasmon resonance (unpublished results) as well as by ^{19}F NMR spectroscopy.[26] Alternatively, structural changes in the chaperone on pilicide binding might induce chemical shift changes for residues not in direct contact with the pilicide. According to X-ray crystallography, binding of peptides to PapD did induce a movement of the two domains in relation to each other, but no rearrangements within either of the domains were observed.[24,35] It therefore appears unlikely that structural changes would explain all the chemical shift changes observed for FimC on binding of pilicides or peptide **11**. Interestingly, PapD and the related chaperone SfaE have been shown to form homodimers,[36,37] and most likely this is also the case for FimC since the structure and function of the three chaperones are almost identical. Thus, PapD forms a weakly bound homodimer that protects the subunit binding area of the chaperone, in particular the F1–G1 loop and the G1 β-strand. If pilicide binding interferes with FimC homodimerization, chemical shift changes would occur throughout the interaction surface. Indeed, T_2 relaxation times, derived from $T_{1\rho}$ measurements, indicated that fast exchange between monomeric FimC and a small amount of FimC homodimer exists. A general increase of about 6% in T_2 relaxation time is observed for FimC in the presence of the PapG peptide **11**, a result that is consistent with a reduction in the amount of homodimer found in solution. The increase in T_2 relaxation time is particularly noticeable in the flexible F1-G1 loop of FimC, a region that undergoes a rigidification in the PapD homodimer. It should be noted that many of the "unexpected" shift changes observed in the presence of peptide **11**, or the pilicides, originate from residues adjacent to the F1–G1 loop and the G1 β-strand, or from other residues that would be affected by FimC homodimerization. It thus appears that these shift changes may well be secondary effects from disruption of FimC homodimerization. However, as indicated previously

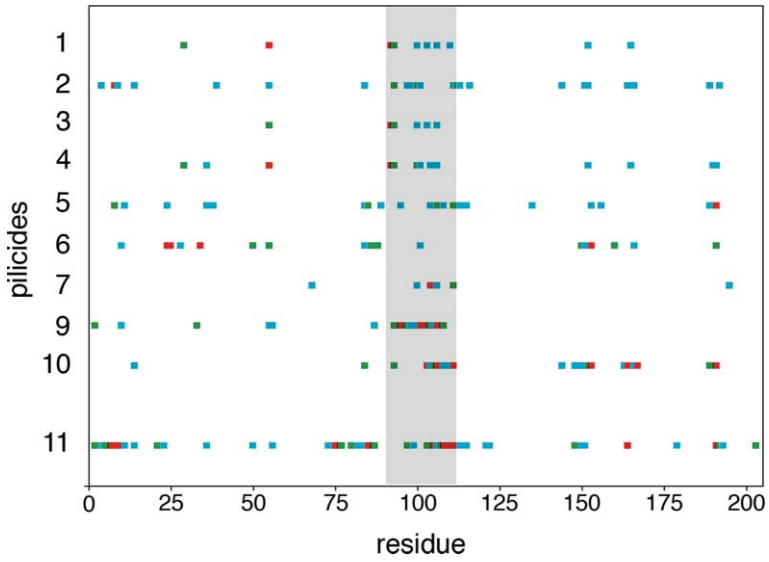

Fig. 4 FimC residues for which a change in the chemical shift of the backbone amide resonances was detected in the presence of pilicides **1–7**, **9**, **10**, or peptide **11**, are marked as a function of the primary sequence of FimC. Δ-Values smaller than 0.003 were omitted. Δ-Values <0.01 are marked in light blue, values for which $0.01 < \Delta < 0.02$ are marked green and Δ-values >0.02 are red. The grey rectangle includes the F1–G1 loop and G1 β-strand (residues 92–115).

by surface plasmon resonance and ^{19}F NMR spectroscopy,[26] less specific binding of the pilicides to the subunit binding area of FimC most likely also contributes to producing the "unexpected" pattern of affected residues.

Location of binding sites from chemical shift mapping data

The relatively small induced chemical shift changes, together with the fact that not all changes observed might originate from direct contact between pilicide and FimC, make it difficult to pinpoint the binding site(s) for the pilicides on the chaperone directly from the observed Δ-values displayed in Fig. 4. There are, however, distinct differences between the pilicides in the patterns of affected backbone amides, as well as in the magnitude of these changes (the Δ-values). In an attempt to locate pilicide binding sites on FimC, a principal component analysis (PCA)[38,39] was performed on the dataset presented in Fig. 4. PCA is a projection method that reduces the dimensionality of complex datasets by introducing latent variables, or principal components, oriented in such a way that they describe the largest variations within the dataset. The observations, in this case each pilicide, are then projected on the principal components, giving each observation a score-value for each principal component. A score-plot where the scores for each observation are plotted against the principal components gives a good overview of structures, such as grouping of observations, within complex datasets. The effect each original variable, in this case the backbone amides in FimC, has on the principal components can be deduced from a loading-plot, making it possible to interpret the scores obtained for the observations, thereby tracing the positions of the pilicides in the score-plot back to the perturbed residues.

Fourteen of the variables were excluded prior to modeling since they experienced zero or close to zero variance, resulting in a total of 73 variables that were used to calculate the model. This gave two principal components describing 78% of the variation in the dataset. As can be seen in the score plot (Fig. 5a), the pilicides can be divided into three groups, with pyridones **1**, **3** and **4** (marked yellow) in one group and the remaining pyridones **2**, **5**, **6** and **7** (marked red) in another group. Pilicide **9** (marked cyan), which is a tyrosine derivative, is well separated from the other compounds. Pilicide **10**, the other tyrosine derivative, was excluded from the PCA model since it gave rise to larger Δ-values than the included pilicides and would therefore have created a biased model. Compound **10** is, however, located close to the

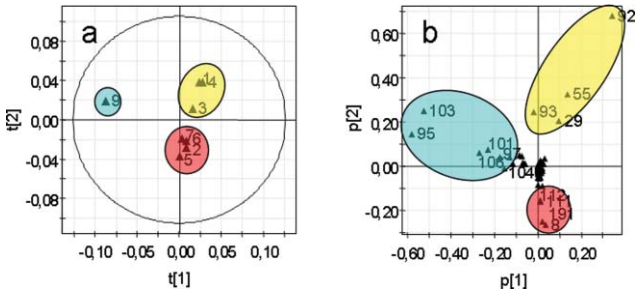

Fig. 5 PCA of the observed chemical shift changes in FimC in the presence of pilicides **1–7** or **9**. (a) Score-plot. The three different groups of pilicides are marked as cyan (**9**), yellow (**1**, **3** and **4**) and red (**2**, **5**, **6** and **7**), respectively. (b) Loading-plot. The FimC residues with the highest impact on the three groups seen in Fig. 5a are marked with the corresponding colours.

structurally related pilicide **9** in a score-plot (data not shown) and therefore interacts in a similar way with FimC as **9**. The separation of the groups marked red and yellow is retained when excluding pilicide **9** from the PCA modelling, thus ruling out that the grouping is induced by this single deviating observation. In the loading plot (Fig. 5b), the FimC residues responsible for the differentiation and grouping of the pilicides are marked, using the same colour coding as in Fig. 5a. It is important to note that the majority of the affected FimC residues are positioned close to the origin in the loading plot. This indicates that most of the observed chemical shift changes (Fig. 4) are independent of pilicide structure and binding site. As discussed above these chemical shift changes most likely originate from reduced homodimerization of FimC, non-specific binding of the pilicides to different parts of the subunit binding area of FimC, or a combination of these two possibilities.

Mapping of the FimC residues that were found to differentiate between the three groups of pilicides in the loading-plot onto the structure of FimC, using the same colour coding as in Fig. 5b, revealed three different sites on the chaperone surface that were affected (Fig. 6). Chemical shift changes involving residues in the cleft could be seen for pilicides **2**, **5**, **6** and **7**. More specifically, **2** and **5** affect residues Arg8, Ile111 and Lys112 (red), while **6** and **7** affect Ile111 and also Asn191. It should be emphasized that Arg8, Ile111 and Lys112 were all strongly affected by the PapG-peptide **11**. Pilicides **1**, **3** and **4** induced chemical shift changes for residues Phe55, Ser92 and Met93 (yellow), whereas

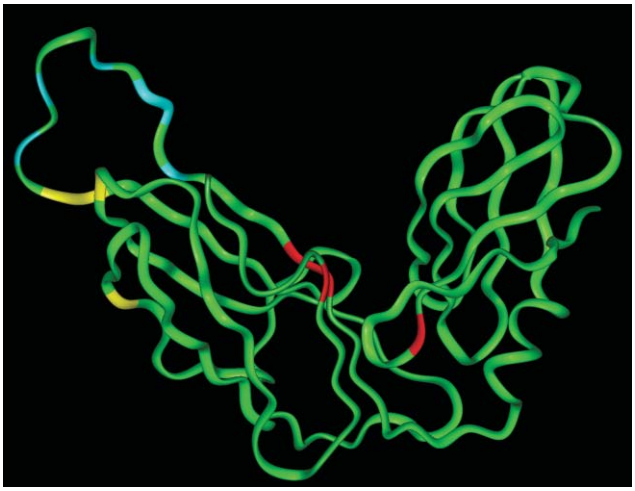

Fig. 6 Mapping of the three different groups of residues involved in binding to pilicides **1–7** and **9** on the three-dimensional structure of FimC.[31] The colour coding is identical to that in Fig. 5b.

Ser29 (yellow) was only affected upon binding of **1** and **4**. These residues are all located on the face of the N-terminal domain of FimC that is opposite to the pilus subunit binding site. No changes are observed for these four residues upon addition of peptide **11** (Fig. 4), confirming that pilicides **1**, **3** and **4** populate a novel binding site. Pilicide **9**, as well as **10**, induces chemical shift changes for Lys95, Lys97, Asn101, Leu103, Gln104 and Ala106 (cyan), residues that are all located in the F1–G1 loop of FimC and that are also affected by peptide **11**. The remaining amino acids located to the left of the origin in the loading-plot (Fig. 5b), that were not considered to be part of the binding site of **9** and **10** (cyan), belong to the F1–G1 loop or adjacent parts of the N-terminal domain.

It is interesting to find that the three structurally different types of pilicides investigated in this study, with one exception, appear to bind to three different sites on FimC. Except for **2**, the disubstituted pyridones (**1**, **3** and **4**) bind to the face of the N-terminal domain of FimC that is opposite to the pilus subunit binding site. The aminomethylated pyridones **5–7**, and disubstituted pyridone **2**, prefer to bind in the cleft, *i.e.* the site for which they were originally designed. Finally, amino acid derivatives **9** and **10** have a preferred binding site in the F1–G1 loop of the N-terminal domain of FimC. As revealed by the chemical shift mapping, all three types of pilicides also affect FimC homodimerization and/or show binding to secondary sites on FimC. It is easy to envision that pilicides binding to the site in the cleft of FimC, or in the F1–G1 loop, would affect homodimerization since these two sites are part of the interactive surface of the homodimer.[36,37] In contrast, the site on the face of the N-terminal domain is opposite to the surface involved in homodimerization and could thus constitute an allosteric site if binding to this site reduces homodimerization. Potentially, binding to this allosteric site could reduce homodimerization by influencing the flexible F1–G1 loop.

Competitive binding of pilicide and PapG peptide

Pilicides, such as the aminomethylated pyridones **5–7** and disubstituted pyridone **2**, that bind in the cleft of FimC should compete with the C-terminal PapG peptide **11** at this site. Aminomethylated pyridone **6** was selected for such a competition study. Upon addition of peptide **11** alone to a sample of ^{15}N-labelled FimC, Arg8 undergoes a large shift, especially in the ^{15}N-dimension (Fig. 7). A large number of other amino acids, such as Thr7, Val9, Leu105, Ile111, Lys112, and Asn191 located in the cleft as well as the residues in the G1 β-strand, are also significantly affected on addition of **11**. Further addition of pilicide **6** to this sample caused Arg8 to move back towards its original position (Fig. 7). This is also the case for the other residues mentioned above. Since addition of pilicide **6** alone to FimC does not affect Arg8, it can safely be concluded that this is an effect of reduced binding of peptide **11**. Thus, pilicide **6** was able to interfere with the binding of peptide **11** despite the fact that **6** only has mM affinity for FimC. This observation provides additional confirmation that aminomethylated pyridones such as **6** bind in the cleft of FimC, just as deduced from the chemical shift mapping study.

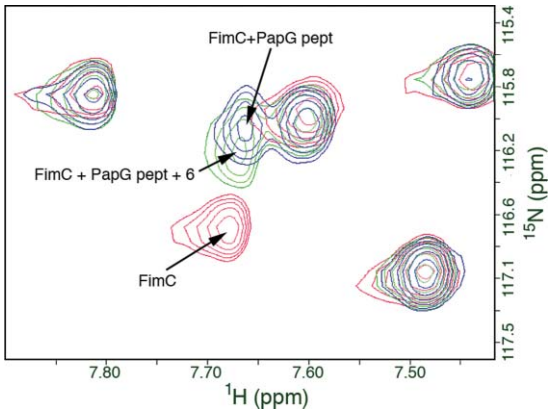

Fig. 7 Part of the ^{15}N-HSQC spectra, showing Arg8 in (i) ^{15}N-FimC (red), (ii) ^{15}N-FimC + one equivalent of PapG peptide **11** (blue), and (iii) ^{15}N-FimC + one equivalent of **11** + ten equivalents of pilicide **6** (green). Pilicide **6** competes with the peptide for the same binding site on FimC since the amide-peak of Arg8 shifts towards its original location on addition of **6**.

Correlation of pilicide binding site with biological data

It is of interest to correlate the information on the preferred binding sites of different types of pilicides with the biological activity of these pilicides. A reduction of the amount of pili present on *E. coli* can be determined as a reduced ability of pilicide treated *E. coli* to agglutinate human erythrocytes, *i.e.* by using a hemagglutination assay. Since hemagglutination is performed on intact *E. coli*, it must be borne in mind that factors such as permeability and uptake may have an effect on the results obtained in this assay. Therefore, it is also important to attempt to find a correlation between the preferred binding site of pilicides and data from a biochemical assay. Such data may be obtained by studying the ability of pilicides to dissociate the native, purified FimC–FimH complex *in vitro*.[18] This assay is based on the fact that the FimC–FimH complex, as well as free FimC, is stable and can be separated and quantified by fast-protein liquid chromatography (FPLC) after incubation with a pilicide. FimH, in contrast, aggregates when dissociated from FimC and is therefore easily separated from FimC and the FimC–FimH complex with FPLC.

Pyridones that prefer to bind in the cleft, *i.e.* disubstituted pyridone **2** and aminomethylated pyridones **5–7**, are unable to dissociate the FimC–FimH complex, or show only a minute activity in this assay (Table 1). Still, some cleft-binders (*e.g.* **2** and **6**) lead to significant reductions of pilus assembly in the *E. coli* as revealed in the hemagglutination assay. It can thus be assumed that the *in vivo* activity observed for pilicides **2** and **5–7** is a result of blocking the chaperone prior to subunit binding in the cleft rather than disruption of FimC–FimH complexes. This agrees well with the fact that the cleft of FimC is inaccessible in the FimC–FimH complex. Initially, it may appear surprising that compounds such as **2** and **5–7** that bind weakly to chaperones are able to interfere with pilus assembly. However, this may be understood from the recent finding that chaperones such as FimC are involved in folding of pilus subunits.[12,13] In particular if the pilicides exert their effect by interfering with one of the early steps in the protein folding pathway this could compensate for their low affinity for FimC. As a consequence

Table 1 Correlation of binding site with the biological activity of pilicides **1–10**, measured as their ability to prevent hemagglutination (HA) and their potency in dissociation of the FimC–FimH complex (CH-diss)

Pilicide	HA[a]	CH-diss[b]	Binding site[c]
1	1	86	Face of N-term. domain
2	3	4	Cleft
3	5	13	Face of N-term. domain
4	—[d]	66	Face of N-term. domain
5	5	0	Cleft
6	3	0	Cleft
7	4	0	Cleft
8[e]	8	0	—
9	8	15	F1–G1 loop
10	8	8	F1–G1 loop

[a] Hemagglutination was determined by addition of the pilicides to a dilution series of *E. coli* strain NU14. The tabulated value refers to the number of two-fold dilutions after which no hemagglutination could be detected. Thus a low value reveals that the pilicide reduces hemagglutination to a high extent (*cf.* the negative control **8** which has a HA value of 8). [b] Each pilicide was incubated with the FimC–FimH complex for 1 h at 37 °C using a pilicide : FimC–FimH ratio of 150 : 1. The fraction of FimC–FimH complex that was dissociated was then determined by FPLC. [c] Residues in the binding site denoted "Face of N-term domain" are marked yellow in Fig. 6. Those in the "Cleft" binding site are red, and those in the "F1–G1 loop" site are blue. [d] Not measured. [e] Negative control. Does not bind to PapD or FimC according to surface plasmon resonance studies. The same values for HA and CH-diss were obtained in the absence of pilicide as in the presence of **8**.

pilus subunits misfold and are directed towards pathways leading to degradation, resulting in an overall reduction in the level of pilus assembly. Future studies of the folding pathway of subunits in the presence of pilicide could give support to this hypothesis. Disubstituted pyridones **1** and **4**, which bind to the face of the N-terminal domain of FimC opposite to the subunit binding site, show significant potency in the FimC–FimH complex dissociation assay (Table 1). Incubation with pilicide **1** also leads to a large reduction in pilus assembly, as determined in the hemagglutination assay. In fact **1** is the most potent pilicide in both assays, which may reflect the observation that **1** binds approximately one order of magnitude stronger to FimC than the other pyridone-based pilicides used in this study. As discussed above, the binding site on the face of the N-terminal domain of FimC may constitute an allosteric site which influences the flexible F1–G1 loop. A reorientation of the F1–G1 loop, which is part of the pilus subunit binding site on FimC, may thus interfere with the protein folding pathway of pilus subunits, and reduce pilus assembly. As revealed by the potency of pyridones **1** and **4** in the FimC–FimH complex dissociation assay, binding to this site also appears to trigger release of pilus subunits from the chaperone before these reach the usher, *i.e.* the pilus assembly platform in the outer cell membrane of the bacterium. Amino acid derivatives **9** and **10**, which bind to the F1–G1 loop of FimC, show only weak activity in the FimC–FimH complex dissociation assay and do not reduce piliation, as determined in the hemagglutination assay. The low potency in the FimC–FimH complex dissociation assay may reflect the affinity of these two pilicides for FimC, a value which could not be determined by NMR spectroscopy. A low affinity for FimC, and possibly also a low uptake into the bacterial periplasm, may contribute to the lack of influence of **9** and **10** on pilus assembly, as determined in the hemagglutination assay.

Conclusions

Compounds termed pilicides have earlier been shown to bind to the periplasmic chaperones PapD and FimC from uropathogenic *E. coli* using surface plasmon resonance and ^{19}F NMR spectroscopy.[18,19,26] In the present study, relaxation-edited ^{1}H NMR spectroscopy was used to confirm the affinity of a selected set of pilicides for the PapD chaperone. Extension of the relaxation edited experiments using spin lock times of variable lengths enabled measurement of the effective transverse relaxation rates of the pilicides in the presence of PapD. From these data, the dissociation constants of the chaperone–pilicide complexes were estimated to be in the mM range. Chemical shift mapping using ^{15}N-labelled FimC was conducted to locate the binding sites for pilicides on FimC. Through principal component analysis of the chemical shift differences observed for the backbone amide groups upon addition of pilicide, three different interaction sites could be distinguished. One binding site is located in the cleft between the two domains of FimC, another one in the F1–G1 loop, and a third one on the face of the N-terminal domain opposite to the pilus subunit binding site. A large part of the observed chemical shift changes in FimC are independent of the structure of the added pilicide and cover an area that, in the closely related chaperone PapD, has been shown to be involved in chaperone homodimerization. Measurement of T_2 relaxation times for FimC in the presence and absence of the C-terminal peptide from the PapG subunit suggested that a small amount of homodimer is present for FimC as well. It could thus be reasoned that a large part of the observed chemical shift changes could be related to pilicide induced disruption of FimC–FimC interactions, although it cannot be ruled out that unspecific binding of pilicides occurs to the same area. Correlation of the ability of pilicides to dissociate FimC–FimH complexes *in vitro*, and their ability to reduce the amount of pili formed by *E. coli*, with their preference for binding at the three sites allowed us to speculate in their mode of action. We propose that pilicides influence pilus formation in *E. coli* either by binding in the cleft of the chaperone, or by influencing the orientation of the flexible F1–G1 loop, both of which are part of the surface by which the chaperone forms complexes with pilus subunits. In addition, we suggest that both these modes of action reduce pilus assembly by interfering with folding of the pilus subunits, which takes place during formation of the chaperone–subunit complexes. Finally, pilicides that influence the F1–G1 loop also appear to reduce pilus formation through their ability to dissociate native chaperone–subunit complexes.

Experimental

Expression and purification of FimC

E. coli strain BL21(DE3)pLys harbouring a modified pACA plasmid was grown overnight on agar-plates at 37 °C. A culture of M9 minimal media containing either ^{15}N–NH_4Cl (1 g L^{-1}) or both ^{15}N–NH_4Cl and ^{13}C-glucose (4 g L^{-1}) was then inoculated and the cells were grown at 37 °C until OD_{600} 0.6 was reached. The cells were then induced with IPTG, grown for 16 h at 23 °C and harvested. After centrifugation, the bacteria were resuspended in Tris buffer (40 mL, 50 mM, 150 mM NaCl, 5 mM EDTA, pH 7.5). Polymyxin-B-sulfate (50 mg in 10 mL of Tris buffer) was added and the suspension was stirred for 2 h at room temperature. The sample was centrifugated and the supernatant (the periplasmic extract) was dialyzed against Tris buffer (10 mM, pH 8.0). The sample was centrifugated again before purification since a small amount of precipitation was observed. Purification was performed on an ÄKTA-system (Amersham Biosciences). The sample was first applied on a DEAE column that was eluted with Tris buffer (10 mM, pH 8.0). It was then applied to a CM column and the protein was eluted with a linear NaCl gradient (0–0.5 M). The fractions were pooled and dialyzed against phosphate buffer (50 mM, pH 5.9). All media contained chloroamphenicol. The yield of purified FimC was 8 mg L^{-1} of bacterial culture.

NMR sample preparation and spectral processing

For the relaxation-edited spectra, each sample was prepared from stock solutions of pilicide and 1-naphthyl acetic acid in

DMSO-d_6 that were added to a PapD solution in phosphate buffer (50 mM, pH 5.9) to yield a final concentration of PapD, 1-naphthyl acetic acid and pilicide of 95 μM. Additional DMSO-d_6 was added so that the DMSO-d_6 content was 5%. A 200 ms cpmg spin-lock was used to efficiently remove the signals from PapD and bound pilicide. All spectra were recorded at 25 °C on a Bruker DRX 400 MHz or a Bruker AMX 500 MHz spectrometer. Processing was conducted in XWINNMR (Bruker).

Triple-resonance experiments, and sensitivity improved gradient selective ^{15}N-HSQC experiments for the chemical shift mapping, were recorded on a Bruker DRX 600 MHz spectrometer equipped with a cryoprobe at 38 °C and pH 5.9. The CBCA(CO)NH experiment was recorded with 91(t_1) × 64(t_2) × 1024(t_3) complex points and the CBCANH experiment with 50(t_1) × 48(t_2) × 1024(t_3) complex data points. The concentration of pilicide and ^{15}N-labelled FimC was 0.1 mM in the samples of pilicides **1–5** and **8–10**. Spectra for **6** and **7** were acquired with a pilicide and ^{15}N-labelled FimC concentration of 36 μM. In order to ensure full solubility of the pilicide, DMSO-d_6 was added to the samples containing pilicides **1–4** and **8** to give a final content of 5%. Subsequently, three different reference-spectra were recorded, one with 0.1 mM ^{15}N-labelled FimC, the second one with 36 μM ^{15}N-labelled FimC and a third with 0.1 mM ^{15}N-labelled FimC containing 5% DMSO-d_6. All ^{15}N-HSQC experiments were recorded with 2048 data points in t_2 and 512 increments in t_1. Processing and peak picking were performed in Felix (Accelrys Inc).

Estimation of K_D of selected pilicides bound to PapD

The R_2 relaxation rates are obtained as a weighted average between the values for the free ligand and the protein–ligand complex and can be expressed as

$$R_{2obs} = P_L R_{2L} + P_{EL} R_{2EL} \quad (1)$$

where R_{2obs} is the observed relaxation rate, P_L and R_{2L} are the population of free pilicide and the relaxation rate of the free pilicide, whereas P_{EL} and R_{2EL} are the population of the PapD–ligand complex and the relaxation rate of the complex. R_{2EL} can be approximated to the R_2 for free PapD due to the large difference in molecular weight of PapD and the pilicides. R_2 for the free pilicides, PapD and the complexes were all determined by line fitting of eqn. (2) to the experimental data.

$$I = I_0 e^{-R2\tau} \quad (2)$$

In eqn. (2), I is the signal intensity of a certain resonance when applying a cpmg spin lock of time τ, and I_0 is the signal intensity at $\tau = 0$.

K_D is defined as

$$K_D = [E][L]/[EL] \quad (3)$$

Since a 1 : 1 ratio between pilicide and PapD was used, eqn. 3 can be rewritten as

$$K_D = (P_L[L_0])^2/((1 - P_L)[L_0]) \quad (4)$$

where L_0 is the total pilicide concentration. The K_D values were estimated from a single pilicide : PapD ratio of 1 : 1.

Chemical shift mapping

The chemical shift mapping experiments were carried out as follows: (i) a reference ^{15}N-HSQC spectrum of ^{15}N-labelled FimC was acquired at 38 °C in buffered aqueous solution at pH 5.9 followed by the corresponding spectrum after addition of one equivalent of pilicide (samples contained DMSO-d_6 as described above, *cf.* NMR sample preparation and spectral processing); (ii) peak picking and assignment of ^{1}H–^{15}N cross peaks was performed in both spectra; (iii) a weighted average of the chemical shift changes in both the ^{1}H- and ^{15}N-dimension for each backbone amide group was calculated according to

$$\Delta = ((^1H_f - {}^1H_b)^2 + 0.2*(^{15}N_f - {}^{15}N_b)^2)^{1/2}$$

where ^1H_f and ^1H_b are the chemical shifts for the amide proton in its free and bound form, respectively. Likewise, $^{15}N_f$ and $^{15}N_b$ are the chemical shifts for the amide nitrogen in its free and bound form; (iv) residues having backbone amide groups that were affected by the pilicides were plotted against the amino acid sequence to get an overview of affected areas of the chaperone. Δ-Values were subjected to principal component analysis (PCA) in order to obtain a comprehensive overview of how the binding of the different pilicides perturbed the chemical shifts of the chaperone.

PCA

Principal component analysis was used to compress the dataset consisting of 9 observations (pilicides **1–9**) and 73 variables (chemical shift changes for backbone amides). Simca-P+ v. 10.0 was used for the PCA-analysis.[40] The variables were centred by subtraction of their mean value before modelling. Eigenvalues larger than 2 were used as a criterion for the number of significant components. Two principal components were calculated with eigenvalues of 3.71 and 2.56, respectively.

FimC–FimH complex dissociation assay

Pilicides **1–9**, and peptide **10**, were dissolved in a 1 : 4 mixture of DMSO and MES buffer (20 mM, pH 6.8) to give a 4.8 mM pilicide stock solution. The pilicide stock solution (200 μL) was diluted with MES buffer (pH 5.8, 350 μL) and then a solution of the FimC–FimH complex[41] in MES buffer (25 μL, 14.2 mg FimC–FimH complex mL^{-1}) was added. This gave a 150 : 1 ratio between pilicide and the FimC–FimH complex. Control solutions were prepared in the same manner, but without pilicide. After incubation of the resulting solutions for 1 h at 37 °C, the amounts of the FimC–FimH complex and free FimC were determined by cation exchange chromatography on a Resource S column (1 mL) using an ÄKTA explorer FPLC (Amersham-Pharmacia). This was done by injecting a sample of the incubated solution (500 μL) on the column and eluting with a gradient of 0–30% of B in A over 8 min (eluent A: 20 mM MES buffer, pH 5.8. Eluent B: 20 mM MES buffer, pH 5.8, containing 0.5 M NaCl. Flow rate of 1.5 mL min^{-1}). The FimC–FimH complex elutes at 40 mM NaCl and free FimC comes at 75 mM NaCl. Integration of peak areas was performed using the ÄKTA Unicorn software. The dissociation of the FimC–FimH complex was calculated by dividing the peak areas for the FimC–FimH complex obtained in presence of a pilicide by that of the control solution.

Hemagglutination assay

E. coli were grown statically for 48 hours and passaged for another 48 hours of static growth in Luria Broth in the presence of 3.6 mM pilicide. This preparation was then used for determination of HA titers as described previously[42] using guinea pig red blood cells.

Acknowledgements

This work was founded by grants from the Swedish Research Council and the Göran Gustafsson Foundation for Research in Natural Sciences and Medicine.

References

1 G. E. Soto and S. J. Hultgren, *J. Bacteriol.*, 1999, **181**, 1059–1071.
2 C. H. Jones, J. S. Pinkner, R. Roth, J. Heuser, A. V. Nicholes, S. N. Abraham and S. J. Hultgren, *Proc. Natl. Acad. Sci. U. S. A.*, 1995, **92**, 2081–2085.
3 S. N. Abraham, D. Sun, J. B. Dale and E. H. Beachey, *Nature*, 1988, **336**, 682.

4 M. J. Kuehn, J. Heuser, S. Normark and S. J. Hultgren, *Nature*, 1992, **356**, 252–255.
5 K. Bock, M. E. Breimer, A. Brignole, G. C. Hansson, K.-A. Karlsson, G. Larsson, H. Leffler, B. E. Samuelsson, N. Strömberg, C. Svanborg-Edén and J. Thurin, *J. Biol. Chem.*, 1985, **260**, 8545–8551.
6 S. J. Hultgren, F. Lindberg, G. Magnusson, J. Kihlberg, J. M. Tennent and S. Normark, *Proc. Natl. Acad. Sci. U. S. A.*, 1989, **86**, 4357–4361.
7 K. W. Dodson, J. S. Pinkner, T. Rose, G. Magnusson, S. J. Hultgren and G. Waksman, *Cell*, 2001, **105**, 733–743.
8 D. G. Thanassi, E. T. Saulino and S. J. Hultgren, *Curr. Opin. Microbiol.*, 1998, **1**, 223–231.
9 A. Holmgren and C.-I. Bränden, *Nature*, 1989, **342**, 248–251.
10 M. Pellechia, P. Güntert, R. Glockshuber and K. Wüthrich, *Nat. Struct. Mol. Biol.*, 1998, **5**, 885–890.
11 C. H. Jones, J. S. Pinkner, A. V. Nicholes, L. N. Slonim, S. N. Abraham and S. J. Hultgren, *Proc. Natl. Acad. Sci. U. S. A.*, 1993, **90**, 8397–8401.
12 J. G. Bann, J. S. Pinkner, C. Frieden and S. J. Hultgren, *Proc. Natl. Acad. Sci. U. S. A.*, 2004, **101**, 17389–17393.
13 M. Vetsch, C. Puorger, T. Spirig, U. Grauschopf, E. U. Weber-Ban and R. Glockshuber, *Science*, 2004, **431**, 329–332.
14 D. Choudhury, A. Thompson, V. Stojanoff, S. Langermann, J. Pinkner, S. J. Hultgren and S. D. Knight, *Science*, 1999, **285**, 1061–1066.
15 F. G. Sauer, K. Fütterer, J. S. Pinkner, K. W. Dodson, S. J. Hultgren and G. Waksman, *Science*, 1999, **285**, 1058–1061.
16 M. M. Barnhart, F. G. Sauer, J. S. Pinkner and S. J. Hultgren, *J. Bacteriol.*, 2003, **185**, 2723–2730.
17 A. Svensson, T. Fex and J. Kihlberg, *J. Comb. Chem.*, 2000, **2**, 736–748.
18 A. Svensson, A. Larsson, H. Emtenäs, M. Hedenstrom, T. Fex, S. J. Hultgren, J. S. Pinkner, F. Almqvist and J. Kihlberg, *ChemBioChem*, 2001, **12**, 915–918.
19 H. Emtenäs, K. Åhlin, J. S. Pinkner, S. J. Hultgren and F. Almqvist, *J. Comb. Chem.*, 2002, **4**, 630–639.
20 N. Pemberton, V. Åberg, H. Almstedt, A. Westermark and F. Almqvist, *J. Org. Chem.*, 2004, **69**, 7830–7835.
21 V. Åberg, M. Hedenström, J. Pinkner, S. Hultgren and F. Almqvist, *Org. Biomol. Chem.*, 2005, **3**, 3886–3892.
22 H. Emtenäs, L. Alderin and F. Almqvist, *J. Org. Chem.*, 2001, **66**, 6756–6761.
23 H. Emtenäs, C. Taflin and F. Almqvist, *Mol. Diversity*, 2003, **7**, 165–169.
24 M. J. Kuehn, D. J. Ogg, J. Kihlberg, L. N. Slonim, K. Flemmer, T. Bergfors and S. J. Hultgren, *Science*, 1993, **262**, 1234–1241.
25 P. J. Hajduk, E. T. Olejniczak and S. W. Fesik, *J. Am. Chem. Soc.*, 1997, **119**, 12257–12261.
26 T. Tengel, T. Fex, H. Emtenäs, F. Almqvist, I. Sethson and J. Kihlberg, *Org. Biomol. Chem.*, 2004, **2**, 725–731.
27 S. B. Shuker, P. J. Hajduk, R. P. Meadows and S. W. Fesik, *Science*, 1996, **274**, 1531–1534.
28 C. Alfano, D. Sanfelice, J. Babon, G. Kelly, A. Jacks, S. Curry and M. R. Conte, *Nat. Struct. Mol. Biol.*, 2004, **11**, 323–329.
29 A. L. Lee, B. F. Volkman, S. A. Robertson, D. Z. Rudner, D. A. Barbash, T. W. Cline, R. Kanaar, D. C. Rio and D. E. Wemmer, *Biochemistry*, 1997, **36**, 14306–14317.
30 M. Pellechia, P. Sebbel, U. Hermanns, K. Wüthrich and R. Glockshuber, *Nat. Struct. Mol. Biol.*, 1999, **6**, 336–339.
31 M. Pellechia, P. Güntert, R. Glockshuber and K. Wütrich, *J. Biomol. NMR*, 1998, **11**, 229–230.
32 S. Grzesiek and A. Bax, *J. Magn. Reson.*, 1992, **99**, 201–207.
33 S. Grzesiek and A. Bax, *J. Am. Chem. Soc.*, 1992, **114**, 6291–6293.
34 D. Muhandriam and L. E. Kay, *J. Magn. Reson., Ser. B*, 1994, **103**, 203–216.
35 G. E. Soto, K. W. Dodson, D. Ogg, C. Liu, J. Heuser, S. D. Knight, J. Kihlberg, C. H. Jones and S. J. Hultgren, *EMBO J.*, 1998, **17**, 6155–6167.
36 D. L. Hung, J. S. Pinkner, S. D. Knight and S. J. Hultgren, *Proc. Natl. Acad. Sci. U. S. A.*, 1999, **96**, 8178–8183.
37 S. D. Knight, D. Choudhury, S. Hultgren, J. Pinkner, V. Stojanoff and A. Thompson, *Acta Crystallogr., Sect. D: Biol. Crystallogr.*, 2002, **D58**, 1016–1022.
38 S. Wold, K. Esbensen and P. Geladi, *Chemom. Intel. Lab. Syst.*, 1987, **2**, 37–52.
39 E. A. Jackson, *A user's guide to principal components*, Wiley, New York, 1991.
40 Umetrics, in 'SIMCA-P+ 10.0.2', Box 7960, S-90719 Umeå, Sweden.
41 M. M. Barnhart, J. S. Pinkner, G. E. Soto, F. G. Sauer, S. Langerman, G. Waksman, C. Frieden and S. J. Hultgren, *Proc. Natl. Acad. Sci. U. S. A.*, 2000, **97**, 7709–7714.
42 L.N. Slonim, J. S. Pinkner, C.-I. Brändén and S. J. Hultgren, *EMBO J.*, 1992, **11**, 4747–4756.